AGU PUBLICATIONS

JGR

Journal of Geophysical Research: Atmospheres

RESEARCH ARTICLE
10.1002/2015JD023178

Key Points:
- Two methods are used to estimate daily mean albedo from MODIS data
- It is the first study to evaluate retrievals of daily mean albedo from MODIS
- Using daily mean albedo reduces bias in shortwave net radiation by 3 W/m^2

Correspondence to:
D. Wang,
ddwang@umd.edu

Citation:
Wang, D., S. Liang, T. He, Y. Yu, C. Schaaf, and Z. Wang (2015), Estimating daily mean land surface albedo from MODIS data, *J. Geophys. Res. Atmos.*, *120*, 4825–4841, doi:10.1002/2015JD023178.

Received 27 JAN 2015
Accepted 2 MAY 2015
Accepted article online 7 MAY 2015
Published online 27 MAY 2015

Estimating daily mean land surface albedo from MODIS data

Dongdong Wang[1], Shunlin Liang[1,2], Tao He[1], Yunyue Yu[3], Crystal Schaaf[4], and Zhuosen Wang[4]

[1]Department of Geographical Sciences, University of Maryland, College Park, Maryland, USA, [2]State Key Laboratory of Remote Sensing Science, School of Geography, Beijing Normal University, Beijing, China, [3]Center for Satellite Applications and Research, National Environmental Satellite, Data, and Information Service, National Oceanic and Atmospheric Administration, College Park, Maryland, USA, [4]Environmental, Earth, and Ocean Sciences, University of Massachusetts Boston, Boston, Massachusetts, USA

Abstract Land surface albedo (LSA) is an important component of the surface radiation budget. For calculation of the surface shortwave net radiation budget, temporal mean albedo is more important than instantaneous albedo. Although Moderate Resolution Imaging Spectroradiometer (MODIS) albedo products have been extensively validated, little effort has been made to evaluate the accuracy of daily mean albedo from MODIS. In this study, we calculate daily mean albedo from MODIS data using a direct method and a look-up table (LUT) method. Comparison with in situ albedo measured at 27 field stations shows that both methods can estimate daily mean albedo with high accuracy. The root-mean-square error (RMSE) of snow-free daily mean albedo retrieved by the LUT method and the direct method is 0.033 and 0.034, respectively. Over the 12 spatially representative stations, RMSE of daily mean albedo is 0.022 and 0.023 by the LUT and direct approach, respectively. Simply using the local noon albedo value as a surrogate of daily mean albedo leads to overestimation of daily shortwave net radiation. By using the data of daily mean albedo, the bias in estimating daily shortwave net radiation can be reduced by 2.8 W/m^2 with the direct method and 2.6 W/m^2 with the LUT method, compared to the use of local noon albedo.

1. Introduction

Land surface albedo (LSA) is an important variable that governs shortwave radiation balance at the land surface by determining the amount of downward shortwave flux reflected back to the atmosphere [*Liang*, 2004]. LSA responds to and interacts with climate variability through various mechanisms. The negative climate forcing of forests resulting from the sequestration of carbon is partially canceled by the low LSA of vegetation canopy [*Betts*, 2000], observed for high latitudes [*Lee et al.*, 2011] and semiarid regions [*Rotenberg and Yakir*, 2010]. The feedback of LSA has played a significant role in the Sahel drought [*Govaerts and Lattanzio*, 2008]. The decreased albedo from retreated snow and sea ice in polar regions is believed to amplify global warming [*Holland and Bitz*, 2003]. The soot present in the snow also reduces the reflectance of snow [*Hansen and Nazarenko*, 2004] and accelerates snowmelt [e.g., *Painter et al.*, 2010]. Thus, LSA is a crucial input value for various climate, mesoscale atmospheric, hydrological, and land surface models [e.g., *Matsumura et al.*, 2010; *Munneke et al.*, 2011; *Qian et al.*, 2011; *Wang and Zeng*, 2010].

LSA is a function of atmospheric parameters, illuminating conditions, and the inherent properties of land surfaces and shows spatial and temporal variations [*Liang et al.*, 2012]. Various retrieval algorithms have been developed to map LSA from satellite data [e.g., *Geiger et al.*, 2008; *Hautecoeur and Leroy*, 1998; *He et al.*, 2012; *Li and Garand*, 1994; *Pinty et al.*, 2000; *Schaaf et al.*, 2002, 2011; *D. D. Wang et al.*, 2013; *Wanner et al.*, 1997]. The bidirectional reflectance distribution function (BRDF) is an important concept for estimating LSA from multiangle satellite data. The quantity of a surface reflecting incident radiation varies according to the illumination and reflecting directions. BRDF provides a mathematical description of the reflectance of the surface as a function of Sun-target-sensor geometry [*Gatebe et al.*, 2003]. Kernel-based BRDF models are generally used to simplify the complex bidirectional reflectance of surfaces with a few kernel parameters [*Roujean et al.*, 1992; *Wanner et al.*, 1997]. Through BRDF models and the corresponding parameters, albedo can be calculated by integrating BRDF weighted by the incident solar radiation.

On the basis of the three-parameter RossThick-LiSparse-Reciprocal model, the Moderate Resolution Imaging Spectroradiometer (MODIS) BRDF/albedo algorithm estimates kernel parameters from the clear-sky surface reflectance of Terra/MODIS and Aqua/MODIS [*Lucht et al*., 2000; *Schaaf et al*., 2002, 2011]. To obtain sufficient samples of surface reflectance over the various angular distributions for modeling BRDF, the MODIS BRDF/albedo algorithm requires temporal aggregation of clear-sky observations within a 16 day period. Standard MODIS Collection V005 BRDF/albedo products have been extensively validated through in situ measurements and high-resolution reference maps over various landscapes [*Cescatti et al*., 2012; *Liu et al*., 2009; *Román et al*., 2009; *Salomon et al*., 2006; *Susaki et al*., 2007; *Wang et al*., 2010, 2004] and have been intercompared with other global LSA products [*He et al*., 2014; *Qin et al*., 2011; *Zhang et al*., 2010].

While the retrieval of the BRDF model parameters (MCD43A1) allows the user to generate albedo quantities at any solar zenith desired, the white-sky albedo (bihemispherical albedo) and black-sky albedo (directional hemispherical albedo) at local solar noon are provided for the convenience of the modeling community (MCD43A3). However, this local solar noon values should be regarded as an instantaneous value and should not be utilized as a surrogate for daily mean albedo. Even under the assumption that surface features are stable, LSA diurnal variations will occur because the illuminating conditions change throughout the day, and thus, the consideration of temporal mean albedos, such as daily mean albedos, is very important for adequately studying the energy balance [*Grant et al*., 2000]. In fact, the use of local noon albedo in calculating daily upward shortwave radiation may produce negative bias as large as −10%, which is much larger than the accuracy requirement of 5% defined by *Global Climate Observing System* [2006].

Although MODIS albedo products have been validated extensively, little effort has been made to evaluate the quality of daily mean albedo from MODIS. In this paper, we used ground measurements at 27 stations to validate MODIS daily mean albedo. Two methods are used to calculate daily mean albedo from MODIS data. By definition, daily mean albedo can be estimated by first calculating instantaneous albedo at various local times from the MODIS BRDF products and then averaging the instantaneous values with the incident radiation as a weight. Besides, we develop a look-up table (LUT) method to estimate daily mean albedo from MODIS data by linking the daily mean value to instantaneous spectral albedos through extensive radiative transfer simulation. Following section 1, section 2 introduces the data used in this paper. The estimation methods of daily mean albedo and related concepts are elaborated in section 3. The results are given in section 4, and section 5 concludes the paper with a brief discussion.

2. Data

MODIS BRDF/albedo (MCD43A) and surface reflectance products (MO/YD09) are the main inputs used in this study. MODIS aerosol products (MO/YD04) are also used in this study to estimate the incident shortwave radiation and the ratio of its diffuse portion. Ground measurements from Surface Radiation Budget Network (SURFRAD) and AmeriFlux are used as ground truth to study the temporal variations in albedo and to validate the satellite albedo retrievals.

2.1. Ground Measurements

Measurements of year 2005 at 27 ground stations from SURFRAD and AmeriFlux are used in the study (Table 1). SURFRAD stations have maintained a good record of surface flux measurement since 1995 and are also contributors to the global Baseline Surface Radiation Network [*Augustine et al*., 2000]. Surface downward and upward shortwave irradiance is recorded every 3 min at seven SURFRAD sites. Two methods are used to measure downward shortwave radiation. The first method directly records it with a single Eppley Precision Spectral Pyranometer. The second method measures its direct and diffuse components with two instruments and calculates downward shortwave radiation as the summation of the two components. The summation method produces higher accuracy than the method using a single pyranometer [*K. Wang et al*., 2013]. The instruments are well calibrated, and the relative uncertainties of measurements are generally within ±5% [*K. Wang et al*., 2012]. AmeriFlux sites are managed by individual investigators and are currently coordinated through the AmeriFlux Management Project of the Department of Energy. Different sites may use slightly different pyranometers to measure shortwave irradiances. The AmeriFlux stations provide downward and upward shortwave irradiance at an interval of 30 min. Instantaneous albedo was simply calculated as the ratio of instantaneous measurements of

Table 1. Information of Ground Measurement Stations Used in the Study

Site Names	Spatially Representative	Network	Latitude	Longitude	No. of Daily Measurement	No. of Noon Measurement
Bondville	N	SURFRAD	40.05	−88.37	364	364
Fort Peck	Y	SURFRAD	48.31	−105.10	363	363
Goodwin Creek	N	SURFRAD	34.25	−89.87	364	364
Desert Rock	Y	SURFRAD	36.63	−116.02	358	358
Penn State	N	SURFRAD	40.72	−77.93	363	364
Sioux Falls	N	SURFRAD	43.73	−96.62	364	364
Table Mountain	Y	SURFRAD	40.13	−105.24	364	364
Southern Great Plains (SGP) Atmospheric Radiation Measurement (ARM) Main	N	AmeriFlux	36.61	−97.49	356	358
Bartlett Experimental Forest	N	AmeriFlux	44.06	−71.29	359	357
Bondville2	N	AmeriFlux	40.01	−88.29	351	348
Brookings	N	AmeriFlux	44.35	−96.84	364	364
Duke Forest Hardwoods	Y	AmeriFlux	35.97	−79.10	365	365
Fermi Agricultural	N	AmeriFlux	41.86	−88.22	168	167
Fermi Prairie	N	AmeriFlux	41.84	−88.24	357	352
Flagstaff Managed Forest	Y	AmeriFlux	35.14	−111.73	118	117
Flagstaff Wildfire	N	AmeriFlux	35.45	−111.77	144	143
Freeman Ranch Mesquite Juniper	Y	AmeriFlux	29.95	−98.00	365	364
Ivotuk	N	AmeriFlux	68.49	−155.75	255	251
Kendall Grassland	Y	AmeriFlux	31.74	−109.94	287	287
Mead Irrigated	N	AmeriFlux	41.17	−96.48	181	365
Mead Rainfed	N	AmeriFlux	41.18	−96.44	168	358
Metolius Intermediate Pine	Y	AmeriFlux	44.45	−121.56	235	236
Morgan Monroe State Forest	Y	AmeriFlux	39.32	−86.41	160	351
UCI_1930	Y	AmeriFlux	55.91	−98.52	134	135
UCI_1989	N	AmeriFlux	55.92	−98.96	265	265
Walker Branch	Y	AmeriFlux	35.96	−84.29	359	359
Willow Creek	Y	AmeriFlux	45.81	−90.08	332	332

upward and downward shortwave irradiance. The total upward and downward shortwave radiations during the daytime were calculated. Daily mean albedo was obtained as the ratio between total upward and total downward shortwave radiations. To obtain sufficient measurements of daily albedo, we also used the measurements of the days when there are missing data. However, the days with valid measurements fewer than half of daytime were not used in the calculation of daily mean albedo. We should note that the quality of satellite albedo retrieval deteriorates with increasing solar zenith angle (SZA) (e.g., dusk and dawn), and the MODIS albedo product is not recommended when SZA is beyond 70° [*Liu et al.*, 2009]. One key issue in validating such coarse-resolution satellite albedo data such as MODIS is the spatial representativeness of ground measurements. High-resolution Landsat data were used to evaluate the spatial homogeneity around the flux tower at each station. The spatially representative analysis of ground measurements was performed by the characteristics of semivariograms [*Román et al.*, 2009, 2010; *Woodcock et al.*, 1988a, 1988b]. Twelve out of the 27 SURFRAD and AmeriFlux stations have relatively homogeneous landscapes, and validation results over these sites will be analyzed and discussed separately.

2.2. MODIS BRDF/Albedo Products

Based on the three-parameter RossThick-LiSparse-Reciprocal model, the MODIS BRDF/albedo algorithm estimates kernel parameters from all clear-sky surface reflectances of Terra/MODIS and Aqua/MODIS observed within a 16 day window [*Schaaf et al.*, 2002]. Because the MODIS sensors measure spectral reflectance over discrete narrow bands, the derived kernel parameters represent the BRDF of these individual narrow bands as well. Linear models are then used to calculate visible, near-infrared, and shortwave broadband BRDF/albedo from spectral BRDF/albedo [*Liang et al.*, 1999]. A backup algorithm is designed to handle the cases where the regular full inversion algorithm fails. The backup algorithm couples the magnitude of any available reflectances with the prior information provided by archetypal BRDF parameters to generate so-called magnitude retrieval. While this method can provide good results, it

is flagged as retrieval from the backup algorithm and should be used with caution [*Liu et al*., 2009]. The suite of MODIS BRDF/albedo products includes the BRDF model parameters, black-sky and white-sky albedos, nadir BRDF-adjusted surface reflectances, and QA flags. The 500 m BRDF parameter products (MCD43A1) and related QA data (MCD43A2) from 2005 covering the 27 ground stations are used in this study.

In addition to the standard MODIS albedo products, *Shuai* [2010] developed two approaches to estimate BRDF/albedo on a daily basis. One method uses 16 day data to invert the kernel-based BRDF models but assigns greater weights to data from days closer to the current day. The other emphasizes the current day's observations by using these data to estimate the magnitude of albedo with the help of BRDF retrieved from the first method. Here we implement a revised version of the second method by replacing the BRDF from the first method with standard MODIS BRDF products (MCD43A1). We refer to the BRDF retrieved from this method as the "1 day corrected" BRDF, whereas the BRDF from the standard MODIS products is known as the "16 day standard" BRDF.

2.3. Other MODIS Products

MODIS daily surface reflectance product will be used in the 1 day corrected method as the current day information to correct the 16 day standard BRDF through dividing the standard BRDF by a ratio between the reflectance from the MODIS reflectance product and the reflectance predicted by the standard BRDF parameters [*Shuai*, 2010]. The daily gridded 500 m products (MOD09GA and MYD09GA) covering the 27 stations during the year 2005 are used in this study [*Vermote et al*., 2002]. Besides, the data of aerosol optical depth (AOD) are also needed to derive the magnitude and distribution of incoming shortwave radiation. The gridded Level 3 daily AOD product (MOD08_D3), which is the average of the MOD04 aerosol values within a $1°\times1°$ grid, is used in this study to reduce the volume of data [*Remer et al*., 2006]. The global data of MOD08_D3 for the year 2005 are downloaded.

3. Methodology

Basic concepts related to daily mean albedo are introduced in this section. The definition of daily mean albedo leads to a direct method of estimating daily mean albedo from explicit integration of instantaneous albedos. Based on radiative transfer simulation with various atmospheric conditions and surface parameters as inputs, we also propose an LUT-based method for estimating the daily mean albedo from instantaneous spectral albedos using the relationship between the two variables.

3.1. Daily Mean Albedo

Albedo is an inherent property of the surface and is influenced by illumination conditions such as spectral and angular distribution of incident solar radiation. The albedo that reflects the actual illumination condition is known as blue-sky albedo. Two conceptual albedo values, black-sky (directional hemispherical reflectance) and white-sky albedos (bihemispherical reflectance), are defined by two ideal illumination scenarios. Isotropic incident radiation from all directions assuming no direct sunlight produces white-sky albedo α^{ws}. Direct radiation from only a given incident solar geometry (Ω_i) defines black-sky albedo $\alpha^{bs}(\Omega_i)$. Blue-sky albedo $\alpha(\Omega_i)$ can be simply calculated from the linear combination of black-sky and white-sky albedos [*Lewis and Barnsley*, 1994]:

$$\alpha(\Omega_i) = \alpha^{ws} p + \alpha^{bs}(\Omega_i)(1-p), \tag{1}$$

where p is the ratio of the surface downward diffuse shortwave radiation to the surface downward total shortwave radiation.

This simple formula assumes the isotropic reflectance of the surface and fails to incorporate multiple scattering between the surface and the atmosphere [*Román et al*., 2010]. *Román et al*. [2010] developed a group of new equations to address these issues. Angular integration is individually applied to each kernel of the kernel-driven BRDF model, and albedo is calculated as the summation of each part [*Román et al*., 2010]:

$$\alpha(\Omega_i) \approx f_0 + f_1 \overline{\overline{K}}''_1(\Omega_i) + f_2 \overline{\overline{K}}''_2(\Omega_i), \tag{2}$$

where f_x is the xth kernel parameter and $K_x(\Omega_v, \Omega_i)$ is its corresponding kernel for a given view geometry Ω_v (i.e., view zenith and azimuth angles) and incident geometry Ω_i (i.e., solar zenith and azimuth angles). f_x is

directly obtained from the MODIS BRDF product, while $K_x(\Omega_v, \Omega_i)$ can be calculated from the RossThick and LiSparse kernel equations. Other components can be calculated as

$$\overline{\overline{K}}_x^{''}(\Omega_i) = (1-p)\overline{K}_x(\Omega_i) + p\overline{\overline{K}}_x^{'}, \tag{3}$$

$$\overline{K}_x(\Omega_v) = \frac{1}{\pi}\int_0^{2\pi}\int_0^1 K_x(\Omega_v, \Omega_i)\mu_i \mathrm{d}\mu_i \mathrm{d}\varphi_i, \tag{4}$$

$$\overline{\overline{K}}_x^{'} = \frac{1}{\pi}\int_0^{2\pi}\int_0^1 \overline{K}_x(\Omega_i)N(\Omega_i)\mu_i \mathrm{d}\mu_i \mathrm{d}\varphi_i, \tag{5}$$

where μ_i is the cosine of the incident zenith angle, φ_i is the incident azimuth angle, and $N(\Omega_i)$ is the normalized sky radiance at an incident geometry. The kernels and the normalized sky radiance can be calculated through radiative transfer simulation, given the Sun-target-sensor geometry and the atmospheric conditions. In practice, these values are calculated offline and stored in an LUT.

The aforementioned albedo refers to the albedo $\alpha(\Omega_i)$ for a given solar geometry Ω_i, which translates to the instantaneous albedo value $\alpha(t)$ at a specific time t. In terms of radiation budget, the average value over a period of time, such as 1 day, carries higher importance. According to the definition of albedo, the daily mean albedo α^{daily} is the ratio between daily upward shortwave radiation E_u^{daily} and daily downward shortwave radiation E_d^{daily} at the surface:

$$\alpha^{\text{daily}} = \frac{E_u^{\text{daily}}}{E_d^{\text{daily}}}. \tag{6}$$

The daily upward energy E_u^{daily} of this equation can be calculated from instantaneous albedo through integration over the daytime:

$$E_u^{\text{daily}} = \int_{\text{daytime}} \alpha(t) I_d(t) \mathrm{d}t, \tag{7}$$

where $I_d(t)$ is the instantaneous downward flux at time t. Since the daily downward radiation can be easily calculated from the integration of $I_d(t)$, the daily mean albedo can be calculated from instantaneous albedo using the following equation:

$$\alpha^{\text{daily}} = \frac{\int_{\text{daytime}} \alpha(t) I_d(t) \mathrm{d}t}{\int_{\text{daytime}} I_d(t) \mathrm{d}t}. \tag{8}$$

In this paper, daily mean albedo is calculated as the average of instantaneous albedos weighted by the instantaneous downward fluxes at each 30 min interval i during the daytime:

$$\alpha^{\text{daily}} = \sum_i [a(t_i) \cdot w(t_i)], \quad \text{and}$$

$$w(t_i) = \frac{I_d(t_i)}{\sum_i I_d(t_i)}. \tag{9}$$

The method of directly estimating daily mean albedo through equation (9) is referred to as the direct method.

3.2. Construction of Daily Mean Albedo LUT

Here we propose an LUT-based method to predict the broadband daily mean blue-sky albedo $\alpha_{\text{broad}}^{\text{daily}}$ from spectral instantaneous black-sky albedo $a_\Lambda^{\text{bs}}(\theta_i)$ for a given SZA θ_i and Band Λ through the following empirical equation:

$$\alpha_{\text{broad}}^{\text{daily}} = c_0 + \sum_{\Lambda=1}^{7} a_\Lambda^{\text{bs}}(\theta_i) \cdot c_\Lambda, \tag{10}$$

where $c_\Lambda(\Lambda = 0, 1, \ldots, 7)$ are regression coefficients. One group of c_Λ are derived for each combination of viewing geometry, AOD, and the length of daytime.

The independent variables on the right-hand side of equation (10) can be easily calculated by using BRDF parameters:

$$\alpha_{\Lambda}^{\mathrm{bs}}(\theta_i) = \frac{1}{\pi}\int_{\varphi=0}^{2\pi}\int_{\mu=0}^{1}\sum_{x=0}^{2}[f_x \bullet K_x(\theta_v, \varphi_v, \theta_i, \varphi_i)]\mu_v \mathrm{d}\mu_v \mathrm{d}\varphi_v, \tag{11}$$

where the subscript *i* refers to the incident solar angles and the subscript *v* refers to the view angles. The left-hand side of equation (10) can be calculated from equation (9) with the broadband instantaneous blue-sky albedo $\alpha_{\mathrm{broad}}(\Omega_{\mathrm{ti}})$. Ω_{ti} is the solar geometry at time ti. Using the method mentioned in section 3.3, $\alpha_{\mathrm{broad}}(\Omega_{\mathrm{ti}})$ is converted from spectral albedo $\alpha_{\Lambda}(\Omega_{\mathrm{ti}})$.

Although equation (10) appears similar to the conversion equation from narrowband albedo to broadband albedo [*Liang*, 2001], some differences are present. Equation (10) is the overarching formula for the LUT-based method to link the broadband daily albedo to spectral instantaneous albedo. To prepare training data sets for estimating coefficients of equation (10), the narrowband-to-broadband conversion coefficients are needed to calculate values of broadband albedo from MODIS spectral albedo data.

The incident solar radiation $I_d(t_i)$ can be modeled as the functions of SZA and AOD through a radiative transfer simulation. MODTRAN 5 (MODerate resolution atmospheric TRANsmission Version 5) [*Berk et al.*, 2004] is used to compute downward shortwave radiation $I_d(\theta_i$, AOD) under various θ_i (0° to 85° in step of 5°) and AOD (0.0 to 1.0 in step of 0.1).

The trajectory of SZA changes during a day is determined by the latitude (LAT) and the Sun's declination angle (DEC) on the day. The atmospheric conditions are assumed to be stable during the day, and a constant AOD value from MODIS is used to represent the atmosphere condition. While we realize that the assumption of a constant AOD throughout a day is idealized, under this assumption, only three coefficients (AOD, DEC, and LAT) in addition to surface BRDF are needed to calculate daily albedo α^{daily}. It should be noted that cloud status may change as well during the day. It will also affect the magnitude and distribution of incoming solar radiation and thus the value of broadband blue-sky albedo.

In Liang's early paper [*Liang*, 2001], a database of surface spectra is used as the input of simulation. Ideally, to consider the anisotropy of surface reflectance, a BRDF database of representative surfaces is needed for calculating albedo. However, no extensive archives of BRDF field measurements are available. As an alternative, in this limited study, the MODIS BRDF retrievals over representative surfaces with the best quality were collected. Three tests were used to assure that the BRDF database selected only the retrievals with the highest quality:

1. *Spatial homogeneity*. Retrieval must originate from a homogeneous pixel. The homogeneous pixels here refer to those with three-by-three neighbors of the same land cover type (using the MODIS International Geosphere-Biosphere Programme land cover MOD12).
2. *High retrieval quality*. Both overall QA (BRDF_Albedo_Quality) and spectral QA (BRDF_Albedo_Band_Quality) flags are used to ensure that retrievals of spectral BRDF are of the highest quality.
3. *Validity of bidirectional reflectance*. The bidirectional reflectance over various geometries is within the valid ranges ([0, 1]).

With the input of these BRDFs as a BRDF database, 10 values of LAT (0° to 90° in step of 10°) and 9 of DEC (−23.5° to 23.5° in step of 5.9°) were used to simulate the diurnal curves of SZA. Together with 11 AOD values (0.0 to 1.0 in step of 0.1) and 18 of SZA (0° to 85° in step of 5°), a total of $18 \times 11 \times 10 \times 9$ scenarios were used. For each scenario, the training data sets of instantaneous spectral albedo and daily mean albedo were calculated from the MODIS BRDF database. Linear regression was then used to obtain a generic set of conversion coefficients across the BRDF types. The coefficients were saved in LUTs for future usage. A climatology value of 0.2 will be used when MODIS (MOD08_D3) fails to produce an AOD value. The day of year (DOY), observation time, and geolocation are required to calculate ancillary parameters such as SZA and DEC. AOD, SZA, DEC, and LAT are then used as an index to interpolate LUT and obtain the proper regression coefficients for the LUT method.

3.3. Narrowband-to-Broadband Conversion

In section 3.1, albedos and other related variables are referred to spectral ones and defined over narrow bands. To obtain broadband albedo for comparison with tower albedometers, the conversion from narrow

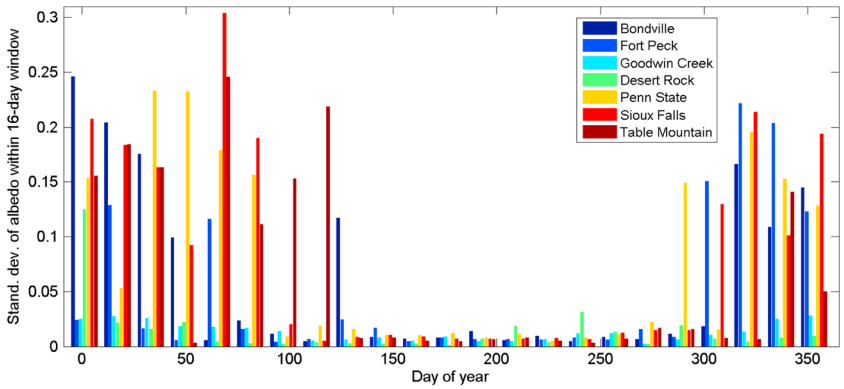

Figure 1. Intraday variability of daily mean albedo at seven SURFRAD sites within 16 day window.

MODIS bands to broadband is needed. Linear regression models are generally established through extensive radiative transfer simulation with representative surface spectra as inputs to facilitate such conversion [*Liang et al*., 1999; *Liang*, 2001].

When discussing conversion coefficients, *Liang et al*. [1999] used two definitions of albedo: apparent albedo and inherent albedo. As shown by its name, apparent albedo is the actual albedo under a given illumination condition and has the same meaning as blue-sky albedo. Thus, in addition to surface reflectance, apparent albedo is also dependent on illumination condition. Inherent albedo can be viewed as black-sky albedo for a particular case of SZA without atmospheric effects. Inherent albedo is an intrinsic property of the surface and independent of atmospheric condition. However, as noted earlier, it is blue-sky albedo (apparent) which should be used for comparison with tower albedometer data and is the quantity used for the calculation of actual surface shortwave net radiation. Thus, the broadband daily mean albedo should also be the weighted average over the day of the broadband instantaneous apparent albedos, and it is the apparent conversion coefficients that are primarily used in this study.

Therefore, we established the conversion coefficients from narrowband apparent albedos to broadband apparent albedo using a similar method to that proposed by *Liang* [2001]. For this study, we ran MODTRAN 5 [*Berk et al*., 2004] for various illumination (SZA) and atmospheric (AOD) conditions, with the U.S. Geological Survey spectra library [*Clark et al*., 2007] used as the inputs of surface reflectance. A set of conversion coefficients was derived for each combination of SZA and AOD.

4. Results

4.1. Variations in Albedo

In situ measurements at SURFRAD sites were analyzed to examine albedo variations. Although QA was applied, spurious measurements remain. The data, in which the daily sum of upward shortwave flux is larger than the daily downward shortwave flux, were excluded from the analysis. The valid daily albedo at the seven sites is first used to demonstrate daily albedo variations within the 16 day window (Figure 1), which is the same length of the retrieval period used by the MODIS albedo algorithm. Snow is a major and significant factor in the daily variation in LSA at these sites. Note that the Collection V005 MODIS standard BRDF/albedo product is only retrieved every 8 days and as such, it underestimates ephemeral snow and is in fact explicitly tuned to retrieve snow-free conditions. For sites at lower latitudes such as Goodwin Creek and Desert Rock, variations were relatively small. At other sites, however, variations were generally smaller during the nonsnow season from mid-May to mid-October than those occurring during the snow season. However, because the magnitudes of surface albedo during the nonsnow season were also small, the coefficient of variation can still be as high as 0.05 during the nonsnow season. This result indicates that incorporation of the current day's observation; thus, capturing both atmospheric variations and snow cover events is needed to adequately capture the day-to-day variations in LSA.

These in situ measurements at the sites are further used to examine differences between use of an instantaneous albedo and of a true daily mean albedo (Figure 2). The two variables show a strong correlation,

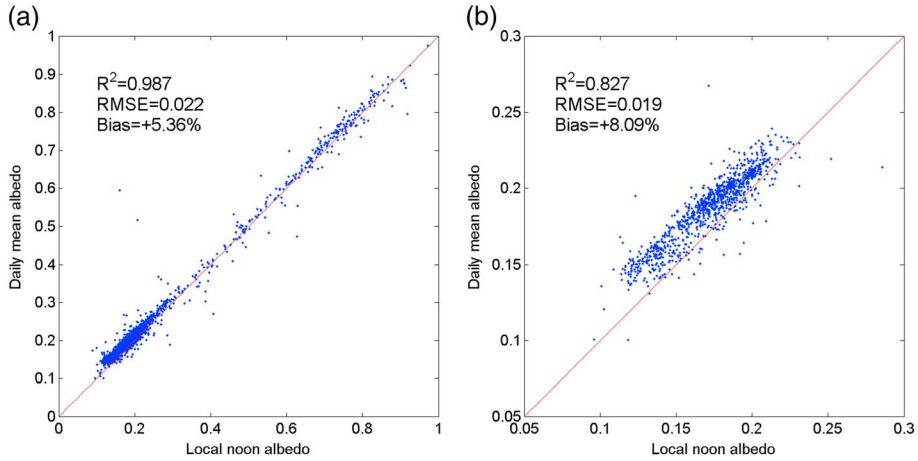

Figure 2. Relationship between daily mean albedo and local noon albedo derived from field measurements at seven SURFRAD sites using (a) all data and (b) snow-free data.

which demonstrates the possibility of predicting daily albedo from instantaneous albedo. The proposed LUT method utilizes this relationship; however, a positive bias is evident across all sites. The average bias for the entire year is +5.4%. After excluding data from the snow seasons (DOY 1–135 and 289–365), the relative difference between daily mean albedo and local noon albedo is as large as 8.1%. The difference at two sites (Fort Peck and Table Mountain) is greater than 10%, which indicates that a 10% underestimation will be introduced when the local noon value is used in calculating daily reflected shortwave radiation. A similar magnitude of difference was detected by *Jacob and Olioso* [2005] at a single French agricultural site, although their results showed that use of instantaneous albedo at local noon ±2 h was closer to the daily mean albedo [*Jacob and Olioso*, 2005].

4.2. An Example of the LUT Model

A total of 17,820 LUT models were constructed to represent various combinations of SZA, AOD, DEC, and LAT. However, only 8305 models were valid because SZA has a lower limit, given LAT and DEC. The parameters of the models were stored in LUT with the four variables (SZA, AOD, DEC, and LAT) as an index. Figure 3 shows the predictability of the model at 0 LAT and 0 DEC. Generally, the broadband daily mean albedo can be reliably predicted from the spectral instantaneous albedo. For the cases where SZA is larger than 70°, uncertainties increase significantly. It indicates that the observations at smaller SZAs are more important for estimating daily mean albedo, because the incoming solar radiation accounts for larger weights for those cases.

4.3. Validation Results

Two methods, direct and LUT, are used to calculate daily mean albedo from AOD and BRDF. Two types of BRDF are used as inputs: the standard MODIS BRDF (16 day standard) products and corrected BRDF (1 day corrected) data. In the 1 day corrected mode, the temporally nearest BRDF retrieval at the same location is used if MODIS BRDF parameters are not successfully retrieved. For each clear-sky observation of MODIS

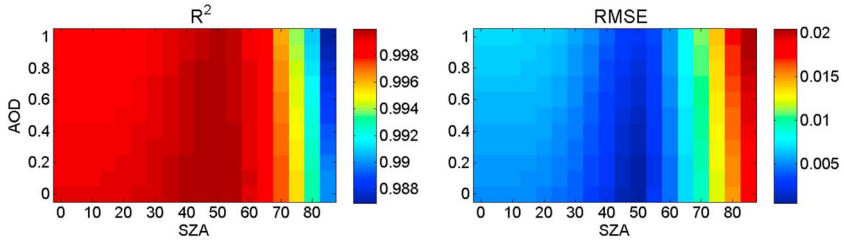

Figure 3. Predictability of the regression models (declination angle = 0° and latitude = 0) from spectral albedos to broadband daily mean albedo in terms of (a) R^2 and (b) RMSE.

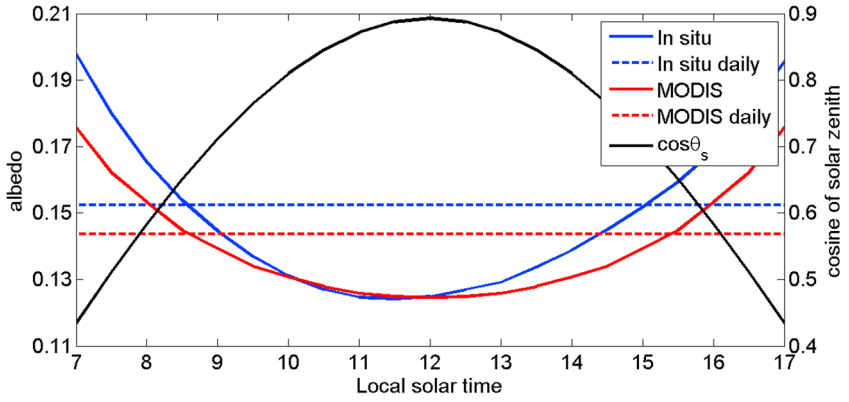

Figure 4. Diurnal change of albedo measured at a SURFRAD site (Fort Peck, 15 July 2005) and retrieved by the direct method from the MODIS data. Cosine of solar zenith angle is also shown, which can roughly indicate the magnitude of incident solar radiation. The blue lines are in situ albedo, whereas the red lines are albedo derived from MODIS. The solid lines refer to instantaneous albedo values throughout the day while the dotted lines are the daily average albedo.

surface reflectance, one daily mean albedo value is calculated. Both MODIS/Terra and MODIS/Aqua surface reflectance products were used in this study. If more than one clear-sky observation is available, the mean of all valid daily mean albedo values is used as the final result. Figure 4 illustrates an example of diurnal change in albedo measured at the Fort Peck station and retrieved from MODIS by the direct method. The daily mean albedo is larger than the local noon albedo due to the bowl shape of diurnal albedo changes. The use of daily mean albedo produces a more accurate estimate of daily surface shortwave budget than does local noon albedo. In this example, albedo is better calculated when the solar zenith angle is small. The discrepancies between field measurements and satellite retrievals increase with solar zenith angle, which is similar to results determined in a previous study [*Liu et al*., 2009]. The field measurements also show albedo in the morning is slightly larger than that in the afternoon. Many factors such as dew and wind speed may result in the asymmetric pattern of diurnal albedo [*Minnis et al*., 1997].

The detailed validation results at the station level are summarized in Table 2. The negative bias of using local noon albedo as a surrogate of daily mean albedo occurs for almost all the sites with only a few exceptions. The daily mean albedo values from both methods agree well with ground measurements. The homogeneous sites generally have smaller errors and biases. For the all-season results, large scattering exists over some homogeneous sites with root-mean-square error (RMSE) greater than 0.05. This is mainly attributed to uncertainties in snow albedo retrieval. It is still a challenge to model snow BRDF with very high accuracy from satellite data, because of such factors as difficulties in atmospheric correction and cloud detection over snow surfaces [*Z. Wang et al*., 2012]. The results of daily mean albedo excluding snow data are also shown (Table 2). With snow albedo data excluded, errors in estimating daily mean albedo have been substantially reduced. Over all the homogenous sites except Metolius Intermediate Pine, the LUT method can estimate daily mean albedo from MODIS with RMSE no greater than 0.025.

Figure 5 shows the overall comparison result between ground measurements and satellite retrievals of local noon and daily mean albedo over all the 27 stations. Even if the stations with less spatial representativeness are included, MODIS can estimate instantaneous (local noon) albedo reliably with a RMSE of 0.050 and a small negative bias of −0.003. The LUT and direct methods can retrieve daily mean albedo with similar accuracy. The LUT approach generates smaller RMSE but slightly greater bias than the direct algorithm. However, if local noon albedo from MODIS is used as the proxy of daily mean albedo, a substantial underestimation exists with a negative bias of −0.017 (−8.8%). Results of snow-free data are separately shown in red. Compared to all-season data, snow-free data have smaller errors but slightly greater negative biases. The underestimation of using local noon albedo as proxy is even more serious, with a bias of −0.021 (−11.9%). In addition to the effects of diurnal changes of albedo, spatial heterogeneity is another important cause of such great underestimation for the snow-free cases. The agreement between MODIS estimates and in situ data is substantially improved, if only the 12 homogeneous stations are used for comparison (Figure 6). For the spatially representative stations, the bias for instantaneous albedo estimation is ignorable. The errors

Table 2. Comparison of Three Retrieved Albedo Values (Local Noon Albedo and Daily Mean Albedo From the Direct and LUT Method, Respectively) With Daily Mean Albedo Measured at the Validation Sites[a]

	Bias (%)			RMSE		
Sites	Noon	Daily (LUT)	Daily (Direct)	Noon	Daily (LUT)	Daily (Direct)
		All Data				
Bondville	−0.061 (−22.1)	−0.048 (−17.4)	−0.046 (−16.7)	0.094	0.088	0.090
Fort Peck	*−0.007 (−3.9)*	*0.008 (4.0)*	*0.012 (6.4)*	*0.045*	*0.057*	*0.045*
Goodwin Creek	−0.063 (−28.7)	−0.049 (−22.3)	−0.050 (−22.9)	0.067	0.055	0.056
Desert Rock	*−0.023 (−11.1)*	*−0.015 (−7.1)*	*−0.012 (−5.6)*	*0.029*	*0.023*	*0.024*
Penn State	−0.045 (−14.8)	−0.032 (−10.5)	−0.032 (−10.5)	0.059	0.052	0.052
Sioux Falls	−0.015 (−5.9)	−0.002 (−0.6)	−0.000 (−0.0)	0.037	0.036	0.037
Table Mountain	*0.004 (2.1)*	*0.016 (9.3)*	*0.023 (13.0)*	*0.047*	*0.051*	*0.060*
ARM SGP Main	−0.017 (−8.5)	−0.004 (−1.9)	−0.006 (−3.0)	0.034	0.030	0.031
Bartlett Experimental Forest	−0.025 (−15.9)	−0.013 (−8.4)	−0.017 (−10.9)	0.047	0.044	0.044
Bondville2	−0.021 (−9.4)	−0.009 (−4.0)	−0.008 (−3.6)	0.045	0.042	0.046
Brookings	0.001 (0.5)	0.020 (8.1)	0.020 (8.4)	0.098	0.112	0.110
Duke Forest Hardwoods	*−0.022 (−14.6)*	*−0.010 (−7.0)*	*−0.012 (−8.2)*	*0.028*	*0.021*	*0.023*
Fermi Agricultural	−0.004 (−1.8)	0.009 (4.2)	0.009 (4.2)	0.039	0.040	0.041
Fermi Prairie	0.012 (6.3)	0.025 (13.3)	0.023 (12.0)	0.066	0.068	0.068
Flagstaff Managed Forest	*0.015 (18.0)*	*0.024 (28.3)*	*0.022 (26.2)*	*0.017*	*0.025*	*0.024*
Flagstaff Wildfire	−0.038 (−25.9)	−0.029 (−19.9)	−0.029 (−19.5)	0.042	0.034	0.034
Freeman Ranch Mesquite Juniper	*−0.024 (−16.0)*	*−0.013 (−8.2)*	*−0.016 (−10.7)*	*0.027*	*0.018*	*0.021*
Ivotuk	−0.007 (−1.8)	0.008 (2.1)	0.011 (2.9)	0.066	0.069	0.069
Kendall Grassland	*−0.025 (−12.8)*	*−0.017 (−8.5)*	*−0.016 (−8.2)*	*0.028*	*0.021*	*0.021*
Mead Irrigated	−0.015 (−7.3)	−0.000 (−0.2)	−0.004 (−2.0)	0.035	0.032	0.035
Mead Rainfed	−0.006 (−2.9)	0.009 (4.5)	0.009 (4.8)	0.027	0.027	0.030
Metolius Intermediate Pine	*−0.022 (−15.9)*	*−0.012 (−8.8)*	*−0.014 (−9.8)*	*0.038*	*0.034*	*0.034*
Morgan Monroe State Forest	*0.000 (0.0)*	*0.012 (8.9)*	*0.009 (6.8)*	*0.015*	*0.020*	*0.020*
UCI_1930	*0.006 (8.3)*	*0.017 (21.6)*	*0.017 (21.2)*	*0.015*	*0.021*	*0.022*
UCI_1989	0.034 (13.5)	0.032 (12.8)	0.044 (17.8)	0.158	0.131	0.164
Walker Branch	*−0.008 (−6.1)*	*0.004 (2.7)*	*0.000 (0.1)*	*0.020*	*0.021*	*0.021*
Willow Creek	*−0.009 (−5.3)*	*0.005 (3.1)*	*−0.001 (−0.8)*	*0.026*	*0.024*	*0.027*
		Snow-Free Data				
Bondville	−0.063 (−26.8)	−0.050 (−21.3)	−0.049 (−21.2)	0.086	0.080	0.081
Fort Peck	*−0.012 (−6.7)*	*0.001 (0.6)*	*0.007 (3.9)*	*0.021*	*0.017*	*0.019*
Goodwin Creek	−0.063 (−28.7)	−0.049 (−22.3)	−0.050 (−22.9)	0.067	0.055	0.056
Desert Rock	*−0.023 (−11.1)*	*−0.015 (−7.1)*	*−0.012 (−5.6)*	*0.029*	*0.023*	*0.024*
Penn State	−0.041 (−19.6)	−0.027 (−12.8)	−0.030 (−14.2)	0.048	0.038	0.042
Sioux Falls	−0.019 (−9.5)	−0.005 (−2.5)	−0.004 (−2.0)	0.034	0.031	0.032
Table Mountain	*−0.004 (−2.8)*	*0.008 (5.1)*	*0.013 (8.4)*	*0.016*	*0.018*	*0.021*
ARM SGP Main	−0.017 (−8.5)	−0.004 (−1.9)	−0.006 (−3.0)	0.034	0.030	0.031
Bartlett Experimental Forest	−0.025 (−15.9)	−0.013 (−8.4)	−0.017 (−10.9)	0.047	0.044	0.044
Bondville2	−0.025 (−12.8)	−0.013 (−6.5)	−0.012 (−6.4)	0.038	0.033	0.037
Brookings	−0.024 (−11.7)	−0.010 (−4.9)	−0.008 (−3.7)	0.038	0.033	0.033
Duke Forest Hardwoods	*−0.022 (−14.6)*	*−0.010 (−7.0)*	*−0.012 (−8.2)*	*0.028*	*0.021*	*0.023*
Fermi Agricultural	−0.009 (−5.4)	0.004 (2.0)	0.003 (1.6)	0.020	0.016	0.018
Fermi Prairie	0.000 (0.1)	0.014 (8.6)	0.011 (6.5)	0.040	0.042	0.040
Flagstaff Managed Forest	*0.015 (18.0)*	*0.024 (28.3)*	*0.022 (26.2)*	*0.017*	*0.025*	*0.024*
Flagstaff Wildfire	−0.038 (−25.9)	−0.029 (−19.9)	−0.029 (−19.5)	0.042	0.034	0.034
Freeman Ranch Mesquite Juniper	*−0.024 (−16.0)*	*−0.013 (−8.2)*	*−0.016 (−10.7)*	*0.027*	*0.018*	*0.021*
Ivotuk	−0.004 (−1.8)	0.015 (7.6)	0.010 (5.2)	0.019	0.025	0.024
Kendall Grassland	*−0.025 (−12.8)*	*−0.017 (−8.5)*	*−0.016 (−8.2)*	*0.028*	*0.021*	*0.021*
Mead Irrigated	−0.018 (−9.2)	−0.003 (−1.6)	−0.007 (−3.6)	0.032	0.028	0.030
Mead Rainfed	−0.008 (−4.5)	0.006 (3.6)	0.006 (3.6)	0.022	0.022	0.023
Metolius Intermediate Pine	*−0.022 (−15.9)*	*−0.012 (−8.8)*	*−0.014 (−9.8)*	*0.038*	*0.034*	*0.034*
Morgan Monroe State Forest	*0.000 (0.0)*	*0.012 (8.9)*	*0.009 (6.8)*	*0.015*	*0.020*	*0.020*
UCI_1930	*0.006 (8.3)*	*0.017 (21.6)*	*0.017 (21.2)*	*0.015*	*0.021*	*0.022*
UCI_1989	−0.013 (−9.5)	−0.003 (−2.2)	−0.005 (−3.9)	0.042	0.032	0.040
Walker Branch	*−0.008 (−6.1)*	*0.004 (2.7)*	*0.000 (0.1)*	*0.020*	*0.021*	*0.021*
Willow Creek	*−0.009 (−5.3)*	*0.005 (3.1)*	*−0.001 (−0.8)*	*0.026*	*0.024*	*0.027*

[a]BRDF is taken from the magnitude inversion using the current day observation. Results in italics are those from the sites with spatial representativeness. The values in parentheses are relative biases.

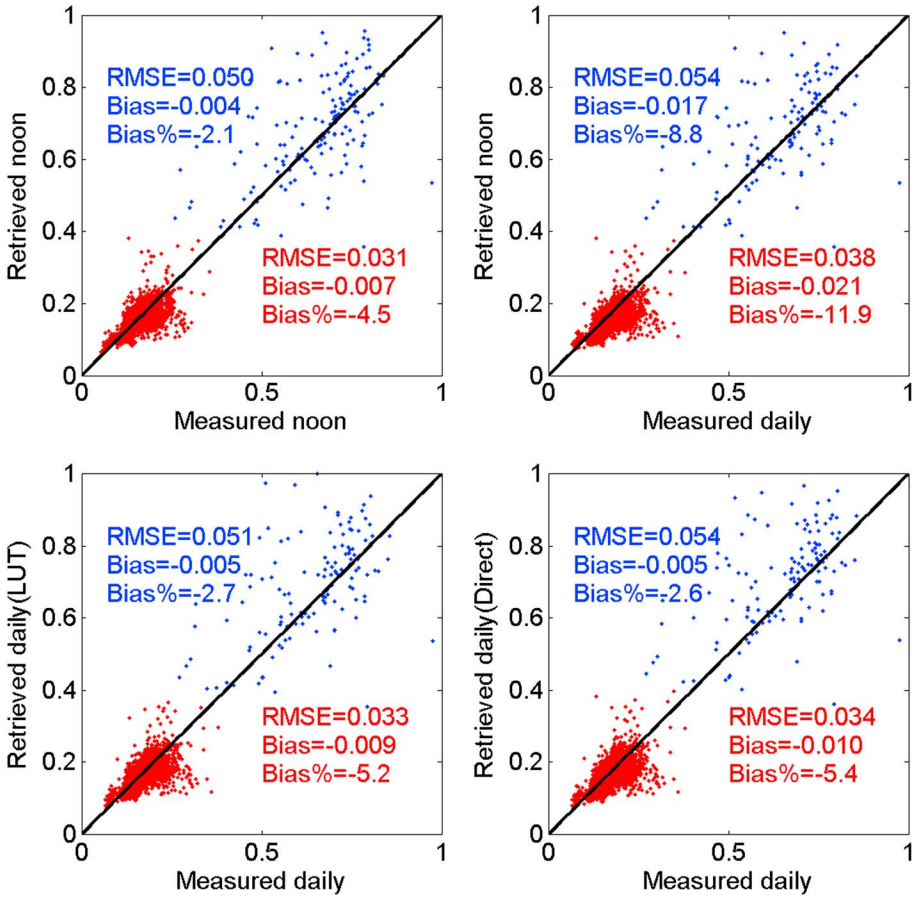

Figure 5. Comparison of instantaneous (local noon) and daily mean albedo from MODIS using various methods with field measurements at all validation sites. Results of snow-free data are shown in red.

of estimating albedo also significantly drop when heterogonous stations are excluded. RMSE of instantaneous albedo is as small as 0.020. However, the negative biases (−9.2%) still exist when comparing MODIS local noon albedo with ground measurements of daily mean albedo. Use of MODIS daily mean albedo will substantially reduce the negative biases by ~7%. Even over the homogeneous sites, both methods slightly underestimate daily mean albedo, given the fact that local noon albedo can be retrieved relatively unbiasedly from MODIS. It is because black-sky albedo with large SZA tends to be underestimated, since MODIS BRDF parameters are not well constrained with observations at large SZA.

The reduction in bias by use of daily mean albedo instead of local noon albedo occurs for all the seasons (Figure 7). There is a systematic difference of ~0.01 between local noon albedo and daily mean albedo. Except in January, daily mean albedo always has smaller absolute bias than local noon albedo. Uncertainties in snow albedo retrievals lead to the opposite results in January. The LUT and direct methods have very similar results. Both can estimate daily mean albedo with bias smaller than 0.01 for 10 out of 12 months. The improvement in RMSE is not as evident as that in bias. The differences in RMSE of the two types of albedo data vary with months. For most of the year, local noon albedo has higher values of RMSE, but the differences are small. The monthly curves of RMSE show a strong seasonal pattern. RMSE is higher for winter seasons when snow is present, while it is lower during the peak growing season when the magnitude of albedo is smaller.

4.4. Impacts of Narrowband-to-Broadband Conversion Coefficients

We studied the influence of narrowband-to-broadband conversion coefficients on the estimation of daily mean albedo (Table 3). In addition to the illumination-dependent coefficients established in section 3.3, we also used the conversion coefficients for inherent albedo [*Liang et al.*, 1999] and apparent albedo

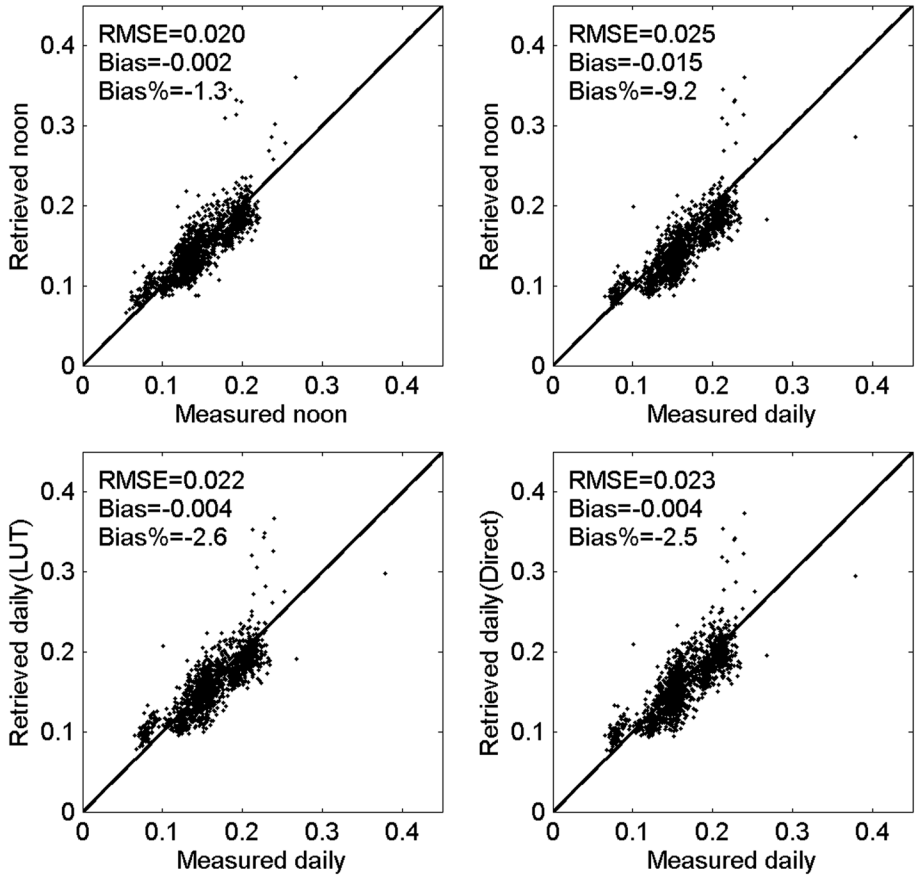

Figure 6. Comparison of instantaneous (local noon) and daily mean snow-free albedo from MODIS using various methods with field measurements at spatially representative sites only.

[*Liang*, 2001]. In theory, the conversion coefficients for apparent albedo should be used when combining blue-sky spectral albedos to broadband values for the comparison with the in situ measurements of broadband actual blue-sky (apparent) albedo (the condition we are considering in this study), while the inherent conversion factors should only be used when combining intrinsic spectral black- and white-sky values to intrinsic (inherent) black and white-sky broadband albedos values (as is done in the production of the MODIS standard products). Furthermore, since apparent albedo is dependent on illumination condition, the conversion coefficients changing with SZA and AOD should theoretically produce better results. In our comparison, however, the three types of coefficients did not result in large differences (Table 3). In terms of RMSE, the inherent and apparent coefficients produced the same results, which were both slightly better than those from the illumination-dependent coefficients.

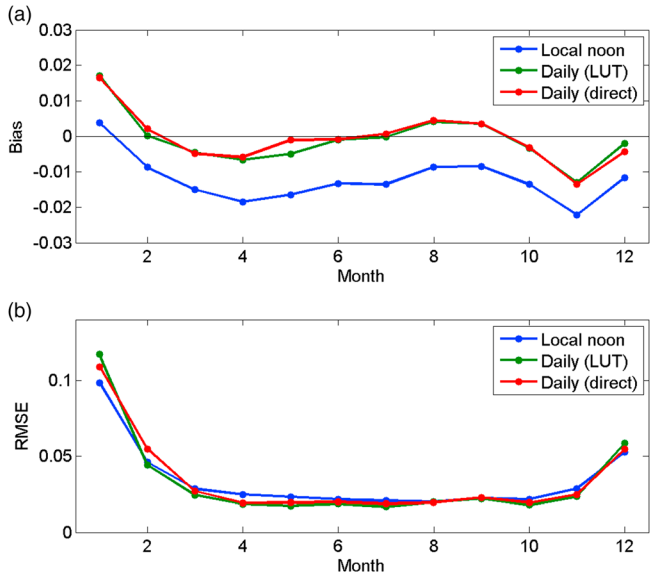

Figure 7. Validation results over spatially representative sites by month for three data sets of albedo, in terms of (a) bias and (b) RMSE.

Table 3. Influence of Narrowband-to-Broadband Conversion Coefficients on the Results of Daily Mean Albedo[a]

	RMSE			Bias		
	Illumination Dependent	Inherent	Apparent	Illumination Dependent	Inherent	Apparent
Bondville	0.042	0.036	0.041	−0.007	−0.014	−0.003
Fort Peck	0.017	0.015	0.021	0.011	0.010	0.017
Goodwin Creek	0.027	0.032	0.023	−0.023	−0.029	−0.019
Desert Rock	0.018	0.014	0.013	−0.012	−0.007	−0.004
Penn State	0.020	0.021	0.017	−0.014	−0.017	−0.008
Sioux Falls	0.018	0.015	0.021	0.010	0.005	0.016
Table Mountain	0.017	0.018	0.021	0.013	0.014	0.019
Mean	0.023	0.022	0.022	−0.003	−0.005	0.003

[a]Three groups of narrowband-to-broadband conversion coefficients are used: illumination dependent, inherent, and apparent. Results are shown for nonsnow season using the direct method with 16 day standard BRDF as inputs.

The inherent coefficients produced very slightly smaller albedo values than the other two apparent coefficients, resulting in slightly larger negative bias.

4.5. Influence on Calculating Surface Radiation Budget

To investigate the influence of different albedo on calculating surface radiation budget, we compared results of daily surface shortwave net radiation calculated from different values of albedo over the 12 homogenous

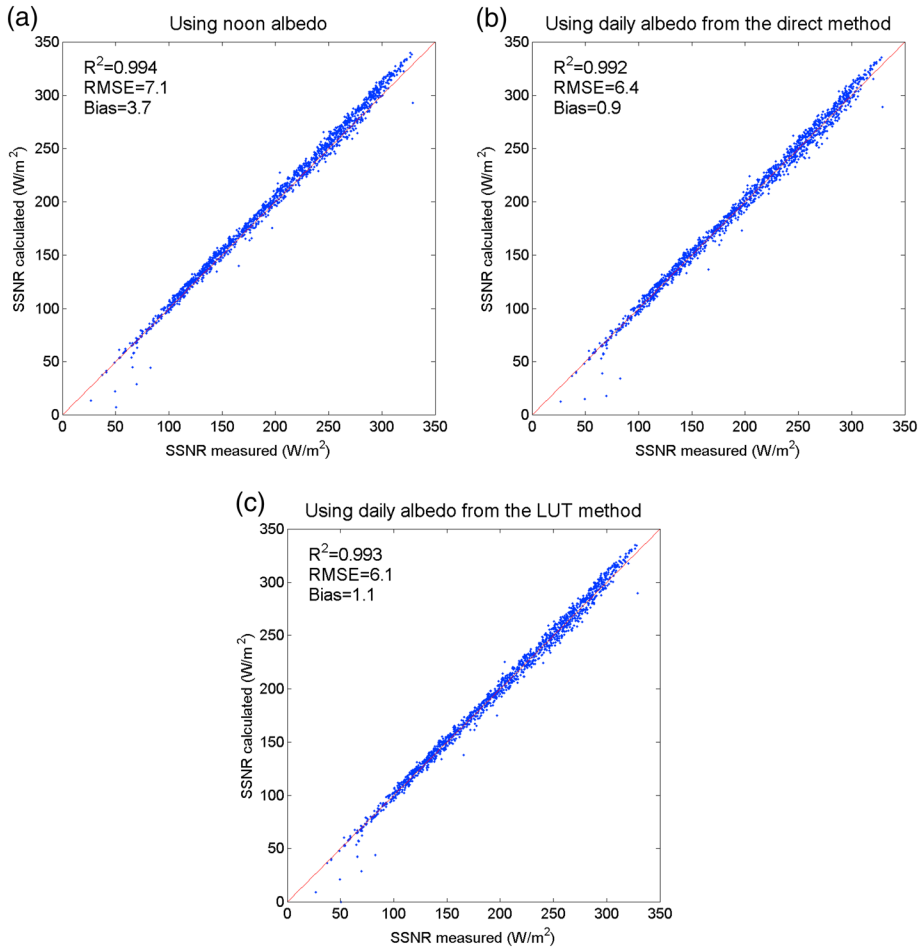

Figure 8. Comparison of surface shortwave net radiation (SSNR) measured at spatially representative sites and SSNR calculated with insolation and albedo from (a) local noon albedo, (b) daily mean albedo from the direct method, and (c) daily mean albedo from the LUT method. The data of the entire year of 2005 are used.

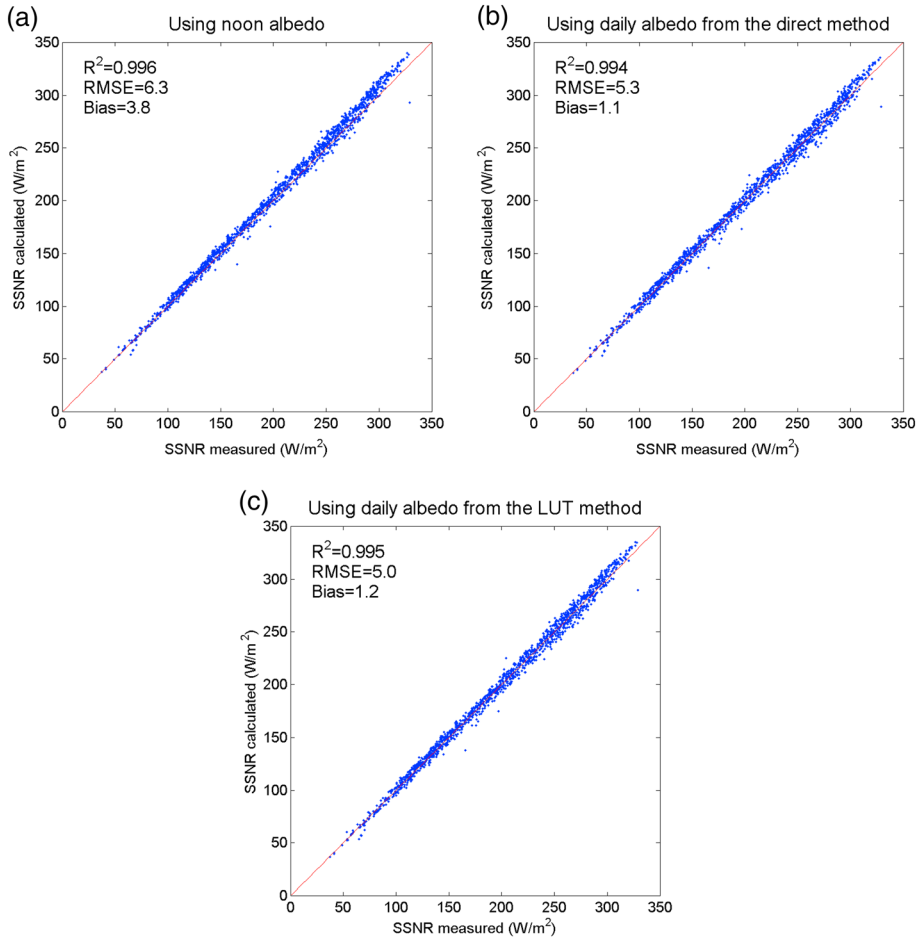

Figure 9. As in Figure 8 but only the snow-free albedo data are used.

stations. The data of surface downward shortwave radiation are taken from ground measurements. Two data sets of surface albedo, local noon albedo, and daily mean albedo are used to calculate daily reflected shortwave radiation. The shortwave net radiation is calculated as the difference between downward and reflected shortwave radiations. The calculated values of daily shortwave net radiation are then compared with the data measured at the ground stations. For the all-season data, using local noon albedo to calculate daily shortwave net radiation will lead to a positive bias of 3.7 W/m^2. The bias is reduced by 2.8 W/m^2 with the direct method and by 2.6 W/m^2 with the LUT method (Figure 8). The direct method produces a smaller bias but a larger RMSE than the LUT method. For the nonsnow data, the reduction of bias in estimating daily shortwave net radiation by using the correct values of albedo has the same magnitude. The bias is reduced from 3.8 W/m^2 to 1.1 W/m^2 by the direct method and to 1.2 W/m^2 by the LUT method (Figure 9). The use of daily mean albedo also reduces the difference (RMSE) between calculated and measured daily shortwave net radiation by 1.0 W/m^2 with the direct method and 1.3 W/m^2 with the LUT method.

5. Conclusion and Discussion

LSA is an important component of surface energy budget. However, current LSA products usually refer to instantaneous albedo. Albedo actually changes with SZA even if the surface property remains constant. In situ measurements from SURFRAD show that daily mean albedo can be 10% larger than local noon albedo during the nonsnow season. Thus, the use of local noon albedo in the calculation of daily surface energy budget leads to underestimation of daily upward shortwave radiation and overestimation of daily net shortwave radiation. Although MODIS instantaneous albedo data have been extensively validated, few

studies have been focused on assessing how reliably daily mean albedo can be retrieved from MODIS. This paper uses two methods to calculate daily mean albedo from MODIS data. The first method computes a weighted average of MODIS instantaneous albedo calculated explicitly from the MODIS BRDF product at each time step throughout a day. The LUT method estimates broadband daily mean albedo from instantaneous spectral albedos using the regression models trained by simulation of atmospheric radiative transfer. The new formulae proposed by *Román et al*. [2010] were used to calculate blue-sky albedo to account for the anisotropy in reflectance and multiple scattering between the surface and the atmosphere. A comprehensive data set of in situ measurements at 7 SURFRAD and 20 AmeriFlux stations is used to evaluate the accuracy of daily mean albedo estimated from MODIS. Validation results suggest that the daily mean albedo retrieved by both the direct and LUT methods are in better agreement with that measured at ground stations than the simple use of the MODIS local noon albedo as a surrogate, with smaller bias and RMSE. This also means better accuracy in calculating daily shortwave net radiation. By using daily mean albedo instead of local noon albedo, the bias in estimating daily shortwave net radiation can be reduced by 2.8 W/m^2.

Current MODIS standard BRDF/albedo products use the multidate approach to gather sufficient observations of surface reflectance over various Sun-target-sensor geometries. However, this assumes that the surface stays relatively stable during the retrieval period. The reflectance of rapidly changing surfaces cannot be captured by such methods. Therefore, estimation of surface albedo from sequential spaceborne sensors presents a challenge in balancing the requirement to aggregate sufficient multiangle observations through the use of a longer time window with the need to capture rapidly changing surfaces with a shorter time window. The MODIS direct broadcast albedo algorithm attempts to meet this challenge by emphasizing the roles of the current day's observations and employing those data for magnitude inversion [*Z. Wang et al*., 2012]. In this study we used a similar 1 day corrected BRDF in estimating daily mean albedo to produce better results in terms of R^2 and RMSE. This is particularly true in rapidly changing conditions, since the current day's information is better equipped to contribute needed spectral and structural information during rapid events such as the snowfall and snowmelt processes. It should be noted that the full inversion of BRDF parameters often fails due to the large variability of surface reflectance caused by the changing surfaces during the composite period. It can be a promising solution to use next-generation geostationary satellite data for such rapidly changing surfaces because of their frequent observations. Another issue with using one observation to adjust BRDF is that a single observation is susceptible to measurement errors, such as failed detection of cloud or cloud shadow, residual atmospheric contaminations. A statistical postprocessing technique, which utilizes information from both climatology and adjacent observations, was developed to address a similar issue [*Liu et al*., 2013].

One important step to estimate shortwave broadband LSA (such as measured from tower-mounted albedometers) from narrowband satellite observations is the narrowband-to-broadband conversion. *Liang et al*. [1999] presented a group of coefficients to convert narrowband inherent albedos to broadband inherent albedo. Because inherent albedo is an intrinsic surface quantity, the conversion coefficients for inherent albedo are useful when discussing the inherent property of the surfaces. The conversion coefficients for apparent albedo are needed in the calculation of the actual instantaneous and daily mean albedo. We established a group of conversion coefficients dependent on SZA and AOD through radiative transfer simulation. However, our validation results showed the use of different types of narrowband-to-broadband conversion coefficients (inherent, apparent, and those changing with SZA and AOD) did not make a significant difference in estimation of daily mean albedo, given the presence of other sources of uncertainty. Note that limited by the availability of spectra database with BRDF information, current narrowband-to-broadband conversion coefficients are based on the assumption of Lambertian surfaces. The simplification of the anisotropy property of surface reflectance contributes further uncertainties in the conversion process.

Although the consideration of diurnal variation in LSA reduces negative bias when comparing the two data sets in this study, small biases can remain between satellite retrievals and field measurements. The mismatch between the footprints of ground measurements and the MODIS pixels can explain some of the differences. After excluding the stations without spatial representativeness, negative biases in MODIS estimates of both instantaneous and daily mean albedo substantially drop. An additional explanation is that the variation in SZA from polar-orbiting satellites is limited. Terra and Aqua overpass the equator within a short window of

local noon (±1.5 h), which indicates that MODIS observations may undersample cases of large SZA and indeed the standard product is not recommended for SZA exceeding 70° [*Liu et al*., 2009]. Nevertheless, the albedo uncertainties for SZA beyond 70° are expected to have limited influence on estimation of daily mean albedo and shortwave net radiation because of the small values of incoming solar radiation for such cases.

Acknowledgments
We gratefully acknowledge the support of NASA and NOAA. We thank SURFRAD and principal investigators of the AmeriFlux stations for making the ground measurement data available. The MODIS albedo, surface reflectance, and aerosol products are available through NASA's Earth Observing System Data and Information System (http://reverb.echo.nasa.gov/). Field measurements of surface radiative fluxes can be found at the websites of SURFRAD (http://www.esrl.noaa.gov/gmd/grad/surfrad/) and AmeriFlux (http://ameriflux.lbl.gov/). We thank the three anonymous reviewers for their valuable and constructive comments and suggestions.

References

Augustine, J. A., J. J. DeLuisi, and C. N. Long (2000), SURFRAD—A national surface radiation budget network for atmospheric research, *Bull. Am. Meteorol. Soc.*, *81*(10), 2341–2357, doi:10.1175/1520-0477(2000)081<2341:sansrb>2.3.co;2.

Berk, A., et al. (2004), MODTRAN5: A reformulated atmospheric band model with auxiliary species and practical multiple scattering options, *Proc. SPIE*, *5425*, 341–347.

Betts, R. A. (2000), Offset of the potential carbon sink from boreal forestation by decreases in surface albedo, *Nature*, *408*(6809), 187–190.

Cescatti, A., et al. (2012), Intercomparison of MODIS albedo retrievals and in situ measurements across the global FLUXNET network, *Remote Sens. Environ.*, *121*, 323–334.

Clark, R. N., G. A. Swayze, R. Wise, E. Livo, T. Hoefen, R. Kokaly, and S. J. Sutley (2007), USGS digital spectral library splib06a, Rep.

Gatebe, C. K., M. D. King, S. Platnick, G. T. Arnold, E. F. Vermote, and B. Schmid (2003), Airborne spectral measurements of surface-atmosphere anisotropy for several surfaces and ecosystems over southern Africa, *J. Geophys. Res.*, *108*(D13), 8489, doi:10.1029/2002JD002397.

Geiger, B., D. Carrer, L. Franchisteguy, J. L. Roujean, and C. Meurey (2008), Land surface albedo derived on a daily basis from Meteosat Second Generation observations, *IEEE Trans. Geosci. Remote Sens.*, *46*(11), 3841–3856, doi:10.1109/tgrs.2008.2001798.

Global Climate Observing System (2006), Systematic observation requirements for satellite-based products for climate, Rep., Geneva, Switzerland.

Govaerts, Y., and A. Lattanzio (2008), Estimation of surface albedo increase during the eighties Sahel drought from Meteosat observations, *Global Planet. Change*, *64*(3–4), 139–145, doi:10.1016/j.gloplacha.2008.04.004.

Grant, I. F., A. J. Prata, and R. P. Cechet (2000), The impact of the diurnal variation of albedo on the remote sensing of the daily mean albedo of grassland, *J. Appl. Meteorol.*, *39*(2), 231–244, doi:10.1175/1520-0450(2000)039<0231:tiotdv>2.0.co;2.

Hansen, J., and L. Nazarenko (2004), Soot climate forcing via snow and ice albedos, *Proc. Natl. Acad. Sci. U.S.A.*, *101*(2), 423–428, doi:10.1073/pnas.2237157100.

Hautecoeur, O., and M. M. Leroy (1998), Surface bidirectional reflectance distribution function observed at global scale by POLDER/ADEOS, *Geophys. Res. Lett.*, *25*(22), 4197–4200, doi:10.1029/1998GL900111.

He, T., S. Liang, D. Wang, H. Wu, Y. Yu, and J. Wang (2012), Estimation of surface albedo and directional reflectance from Moderate Resolution Imaging Spectroradiometer (MODIS) observations, *Remote Sens. Environ.*, *119*, 286–300, doi:10.1016/j.rse.2012.01.004.

He, T., S. Liang, and D.-X. Song (2014), Analysis of global land surface albedo climatology and spatial-temporal variation during 1981–2010 from multiple satellite products, *J. Geophys. Res. Atmos.*, *119*, 10,281–10,298, doi:10.1002/2014JD021667.

Holland, M. M., and C. M. Bitz (2003), Polar amplification of climate change in coupled models, *Clim. Dyn.*, *21*(3–4), 221–232, doi:10.1007/s00382-003-0332-6.

Jacob, F., and A. Olioso (2005), Derivation of diurnal courses of albedo and reflected solar irradiance from airborne POLDER data acquired near solar noon, *J. Geophys. Res.*, *110*, D10104, doi:10.1029/2004JD004888.

Lee, X., et al. (2011), Observed increase in local cooling effect of deforestation at higher latitudes, *Nature*, *479*(7373), 384–387, doi:10.1038/nature10588.

Lewis, P., and M. J. Barnsley (1994), Influence of the sky radiance distribution on various formulations of the earth surface albedo, in *Proc. Mesures Physiques et Signatures en Teledetection*, edited, pp. 707–716, Agence Spatiale Européenne, Val d'Isere, France.

Li, Z. Q., and L. Garand (1994), Estimation of surface albedo from space: A parameterization for global application, *J. Geophys. Res.*, *99*(D4), 8335–8350, doi:10.1029/94JD00225.

Liang, S. (2004), *Quantitative Remote Sensing of Land Surfaces*, John Wiley, Hoboken.

Liang, S., A. H. Strahler, and C. Walthall (1999), Retrieval of land surface albedo from satellite observations: A simulation study, *J. Appl. Meteorol.*, *38*(6), 712–725.

Liang, S., X. Li, and J. Wang (Eds.) (2012), *Advanced Remote Sensing: Terrestrial Information Extraction and Applications*, Academic Press, Amsterdam, Netherlands.

Liang, S. L. (2001), Narrowband to broadband conversions of land surface albedo: I. Algorithms, *Remote Sens. Environ.*, *76*(2), 213–238.

Liu, J. C., C. Schaaf, A. Strahler, Z. T. Jiao, Y. M. Shuai, Q. L. Zhang, M. Roman, J. A. Augustine, and E. G. Dutton (2009), Validation of Moderate Resolution Imaging Spectroradiometer (MODIS) albedo retrieval algorithm: Dependence of albedo on solar zenith angle, *J. Geophys. Res.*, *114*, D01106, doi:10.1029/2008JD009969.

Liu, N. F., Q. Liu, L. Z. Wang, S. L. Liang, J. G. Wen, Y. Qu, and S. H. Liu (2013), A statistics-based temporal filter algorithm to map spatiotemporally continuous shortwave albedo from MODIS data, *Hydrol. Earth Syst. Sci.*, *17*(6), 2121–2129, doi:10.5194/hess-17-2121-2013.

Lucht, W., C. B. Schaaf, and A. H. Strahler (2000), An algorithm for the retrieval of albedo from space using semiempirical BRDF models, *IEEE Trans. Geosci. Remote Sens.*, *38*(2), 977–998, doi:10.1109/36.841980.

Matsumura, S., K. Yamazaki, and T. Tokioka (2010), Summertime land-atmosphere interactions in response to anomalous springtime snow cover in northern Eurasia, *J. Geophys. Res.*, *115*, D20107, doi:10.1029/2009JD012342.

Minnis, P., S. Mayor, W. L. Smith, and D. F. Young (1997), Asymmetry in the diurnal variation of surface albedo, *IEEE Trans. Geosci. Remote Sens.*, *35*(4), 879–891, doi:10.1109/36.602530.

Munneke, P. K., M. R. van den Broeke, J. T. M. Lenaerts, M. G. Flanner, A. S. Gardner, and W. J. van de Berg (2011), A new albedo parameterization for use in climate models over the Antarctic ice sheet, *J. Geophys. Res.*, *116*, D05114, doi:10.1029/2010JD015113.

Painter, T. H., J. S. Deems, J. Belnap, A. F. Hamlet, C. C. Landry, and B. Udall (2010), Response of Colorado River runoff to dust radiative forcing in snow, *Proc. Natl. Acad. Sci. U.S.A.*, *107*(40), 17,125–17,130, doi:10.1073/pnas.0913139107.

Pinty, B., F. Roveda, M. M. Verstraete, N. Gobron, Y. Govaerts, J. V. Martonchik, D. J. Diner, and R. A. Kahn (2000), Surface albedo retrieval from Meteosat: 1. Theory, *J. Geophys. Res.*, *105*(D14), 18,099–18,112, doi:10.1029/2000JD900113.

Qian, Y., M. G. Flanner, L. R. Leung, and W. Wang (2011), Sensitivity studies on the impacts of Tibetan Plateau snowpack pollution on the Asian hydrological cycle and monsoon climate, *Atmos. Chem. Phys.*, *11*(5), 1929–1948, doi:10.5194/acp-11-1929-2011.

Qin, J., K. Yang, S. L. Liang, H. Zhang, Y. M. Ma, X. F. Guo, and Z. Q. Chen (2011), Evaluation of surface albedo from GEWEX-SRB and ISCCP-FD data against validated MODIS product over the Tibetan Plateau, *J. Geophys. Res.*, *116*, D24116, doi:10.1029/2011JD015823.

Remer, A., D. Tanre, Y. Kaufman, R. Levy, and S. Mattoo (2006), Algorithm for remote sensing of tropospheric aerosol from MODIS, Rep.
Román, M. O., et al. (2009), The MODIS (Collection V005) BRDF/albedo product: Assessment of spatial representativeness over forested landscapes, *Remote Sens. Environ.*, *113*(11), 2476–2498, doi:10.1016/j.rse.2009.07.009.
Román, M. O., C. B. Schaaf, P. Lewis, F. Gao, G. P. Anderson, J. L. Privette, A. H. Strahler, C. E. Woodcock, and M. Barnsley (2010), Assessing the coupling between surface albedo derived from MODIS and the fraction of diffuse skylight over spatially-characterized landscapes, *Remote Sens. Environ.*, *114*(4), 738–760, doi:10.1016/j.rse.2009.11.014.
Rotenberg, E., and D. Yakir (2010), Contribution of semi-arid forests to the climate system, *Science*, *327*(5964), 451–454, doi:10.1126/science.1179998.
Roujean, J. L., M. Leroy, and P. Y. Deschamps (1992), A bidirectional reflectance model of the Earth's surface for the correction of remote sensing data, *J. Geophys. Res.*, *97*(D18), 20,455–20,468, doi:10.1029/92JD01411.
Salomon, J. G., C. B. Schaaf, A. H. Strahler, F. Gao, and Y. F. Jin (2006), Validation of the MODIS bidirectional reflectance distribution function and albedo retrievals using combined observations from the Aqua and Terra platforms, *IEEE Trans. Geosci. Remote Sens.*, *44*(6), 1555–1565, doi:10.1109/tgrs.2006.871564.
Schaaf, C. B., et al. (2002), First operational BRDF, albedo nadir reflectance products from MODIS, *Remote Sens. Environ.*, *83*(1–2), 135–148.
Schaaf, C. L. B., J. Liu, F. Gao, and A. H. Strahler (2011), Aqua and Terra MODIS albedo and reflectance anisotropy products, in *Land Remote Sensing and Global Environmental Change: NASA's Earth Observing System and the Science of ASTER and MODIS*, edited by B. Ramachandran, C. Justice, and M. Abrams, Springer, New York.
Shuai, Y. (2010), Tracking daily land surface albedo and reflectance anisotropy with MODerate-Resolution Imaging Spectroradiometer (MODIS), PhD dissertation thesis, Boston Univ.
Susaki, J., Y. Yasuoka, K. Kajiwara, Y. Honda, and K. Hara (2007), Validation of MODIS albedo products of paddy fields in Japan, *IEEE Trans. Geosci. Remote Sens.*, *45*(1), 206–217, doi:10.1109/tgrs.2006.882266.
Vermote, E. F., N. Z. El Saleous, and C. O. Justice (2002), Atmospheric correction of MODIS data in the visible to middle infrared: First results, *Remote Sens. Environ.*, *83*(1–2), 97–111.
Wang, D. D., S. L. Liang, T. He, and Y. Y. Yu (2013), Direct estimation of land surface albedo from VIIRS data: Algorithm improvement and preliminary validation, *J. Geophys. Res. Atmos.*, *118*, 12,577–12,586, doi:10.1002/2013JD020417.
Wang, K., J. Augustine, and R. E. Dickinson (2012), Critical assessment of surface incident solar radiation observations collected by SURFRAD, USCRN and AmeriFlux networks from 1995 to 2011, *J. Geophys. Res.*, *117*, D23105, doi:10.1029/2012JD017945.
Wang, K., S. Liang, C. L. Schaaf, and A. H. Strahler (2010), Evaluation of Moderate Resolution Imaging Spectroradiometer land surface visible and shortwave albedo products at FLUXNET sites, *J. Geophys. Res.*, *115*, D17107, doi:10.1029/2009JD013101.
Wang, K., R. E. Dickinson, Q. Ma, J. A. Augustine, and M. Wild (2013), Measurement methods affect the observed global dimming and brightening, *J. Clim.*, *26*(12), 4112–4120, doi:10.1175/jcli-d-12-00482.1.
Wang, K., J. M. Liu, X. J. Zhou, M. Sparrow, M. Ma, Z. Sun, and W. H. Jiang (2004), Validation of the MODIS global land surface albedo product using ground measurements in a semidesert region on the Tibetan Plateau, *J. Geophys. Res.*, *109*, D05107, doi:10.1029/2003JD004229.
Wang, Z., and X. B. Zeng (2010), Evaluation of snow albedo in land models for weather and climate studies, *J. Appl. Meteorol. Climatol.*, *49*(3), 363–380, doi:10.1175/2009jamc2134.1.
Wang, Z., C. B. Schaaf, M. J. Chopping, A. H. Strahler, J. Wang, M. O. Roman, A. V. Rocha, C. E. Woodcock, and Y. Shuai (2012), Evaluation of Moderate-resolution Imaging Spectroradiometer (MODIS) snow albedo product (MCD43A) over tundra, *Remote Sens. Environ.*, *117*, 264–280, doi:10.1016/j.rse.2011.10.002.
Wanner, W., A. H. Strahler, B. Hu, P. Lewis, J. P. Muller, X. Li, C. L. B. Schaaf, and M. J. Barnsley (1997), Global retrieval of bidirectional reflectance and albedo over land from EOS MODIS and MISR data: Theory and algorithm, *J. Geophys. Res.*, *102*(D14), 17,143–17,161, doi:10.1029/96JD03295.
Woodcock, C. E., A. H. Strahler, and D. L. B. Jupp (1988a), The use of variograms in remote sensing: 2. Real digital images, *Remote Sens. Environ.*, *25*(3), 349–379, doi:10.1016/0034-4257(88)90109-5.
Woodcock, C. E., A. H. Strahler, and D. L. B. Jupp (1988b), The use of variograms in remote sensing: 1. Scene models and simulated images, *Remote Sens. Environ.*, *25*(3), 323–348, doi:10.1016/0034-4257(88)90108-3.
Zhang, X. T., S. L. Liang, K. C. Wang, L. Li, and S. Gui (2010), Analysis of global land surface shortwave broadband albedo from multiple data sources, *IEEE J. Sel. Top. Appl. Earth Obs. Remote Sens.*, *3*(3), 296–305, doi:10.1109/jstars.2010.2049342.